Transfer of information through waveguides near an exceptional point

Nimrod Moiseyev [1,*] and Milan Šindelka[2]

[1]*Schulich Faculty of Chemistry and Faculty of Physics, Technion-Israel Institute of Technology, Haifa 32000, Israel*
[2]*Institute of Plasma Physics, Academy of Sciences of the Czech Republic, Za Slovankou 1782/3, 18200 Prague 8, Czech Republic*

The propagation of light in a pair of waveguides (WGs) with a complex index of refraction is studied, when the WG parameters are adjusted in such a way as to bring the system extremely close to an exceptional point (EP) while slightly breaking $\mathcal{PT}$ symmetry. We find that this breaking of $\mathcal{PT}$ symmetry does not affect the structure of the output signals, although the corresponding propagation constants become slightly complex. Only for sufficiently strong breaking of the $\mathcal{PT}$ symmetry the signal is enhanced or suppressed in a substantial manner. Moreover, due to the EP it is impossible to tap light into another WG and thus read the transmitted signal without destroying completely the nodal structure and changing dramatically the intensity of the signal.

I. INTRODUCTION

Non-Hermitian physical systems have attracted considerable attention during the last decade due to their unconventional behavior induced by the so-called exceptional points (EPs). See, for example, the review of Heiss on the physics of EPs and references therein [1]. Literally hundreds of papers were published in most leading scientific journals on the role of EPs in diverse quantum, optical, and mechanical systems. An impact of this topical concept is documented by the number of recent review papers [2–5] and outlooks [6–8].

In the present article, we focus on highlighting the role of EPs in slightly curved waveguides (WGs) with a slightly broken $\mathcal{PT}$ symmetry. $\mathcal{PT}$-symmetry breaking occurs here due to the fact that the index of refraction, $n(x, z)$, is set up to vary along the propagation axis z, so as to bring the WGs continuously from the standard Hermitian operational regime towards the EP condition and back. To our knowledge, such a WG setup has not been studied before in the literature. We show that an EP does not affect the transfer of optical information through straight WGs. However, the EP has an enormously large effect whenever the originally straight WGs are bent to have the usual structure that allows tapping light from one WG into another WG (as plotted in Fig. 1 below; see also Fig. 2 of Ref. [9] and Fig. 1 of Ref. [10]). We demonstrate that two extreme situations are possible, depending upon the direction of the bending and on the type of the propagated mode. Either the power of the propagated light grows exponentially (and might burn the WGs), or the power of the light at the exit completely vanishes.

$\mathcal{PT}$-symmetric WGs were studied for the first time by Makris *et al.* [11] and by Klaiman *et al.* [12]. Subsequent studies of the subject include Refs. [13–20]. It was shown in Ref. [12] that it is possible to produce a straight gain-and-loss WG in which the propagation constants of all modes are real,

as long as the strength parameter of the imaginary index of refraction, α, is smaller than a critical value. At this critical value, $\alpha_{\rm EP}$, two modes coalesce to form an EP. Theoretical argument of Refs. [11,12] then motivated the milestone experiment published one decade ago [13] that has opened the field of $\mathcal{PT}$ symmetry in optics. For $\alpha > \alpha_{\rm EP}$, complex propagation constants are obtained (see, for example, Fig. 5(b) in the review article [21]).

The subsequent structure of the paper is as follows: In Sec. II, we will formulate the problem mathematically and describe the used computational algorithm. In Sec. III, we introduce our basic WG setup (shown in Fig. 1). In Sec. IV A, we will present the obtained numerically exact results corresponding to straight WGs which possess remarkable physical features due to gradual variation of the index of refraction along the light propagation axis (Figs. 2–6). In Sec. IV B, we will present the obtained numerically exact results corresponding to slightly bent WGs. Namely, in Fig. 7 we demonstrate that bending affects exponentially the strength of the output signal. The output power can either exponentially grow (and it even might burn the WGs), or it can be exponentially suppressed. Finally, we supply concluding remarks in Sec. V. In addition, Appendix A provides a self-contained description of the used scattering formalism (which is properly adapted to our studied situation when the index of refraction is complex valued). Appendix B contains the additional plots complementing the paper. We prefer to include these plots in the form of an Appendix in order to make the overall structure of our article more transparent for the readers.

II. MATHEMATICAL FORMULATION OF THE PROBLEM

The scalar Maxwell equation to be solved takes the form

$$[\partial_{xx} + \omega^2 n^2(x, z) + \partial_{zz}]\Psi(x, z) = 0. \tag{1}$$

One starts with solving the z-adiabatic problem (where z represents a parameter rather than a dynamical coordinate), that
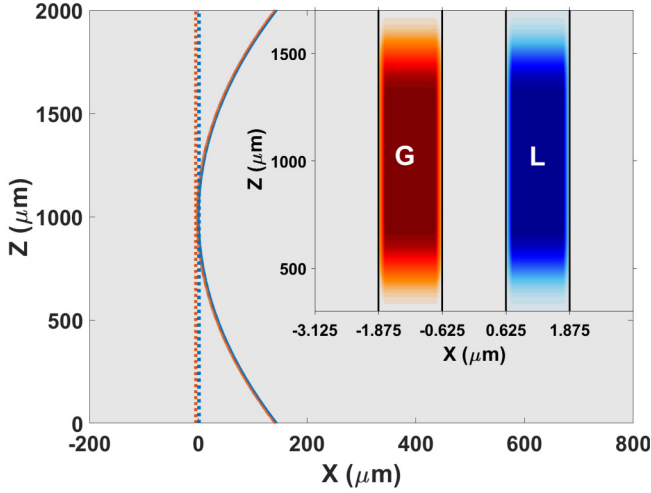
*nimrod@technion.ac.il

FIG. 1. Two coupled waveguides (WGs) with a complex index of refraction. The straight and bent arrangements are denoted respectively by dashed and solid lines (these are two distinct WG setups plotted in the same figure). An inset shows how an imaginary part of the refraction index (responsible for gain and loss) varies along the propagation axis z. Note that this imaginary part is set to vanish at the entrance and exit from the WGs. For more details, see Refs. [12,13,24].

is,

$$[\partial_{xx} + \omega^2 n^2(x, z)]\phi_\nu(x, z) = \beta_\nu^2(z)\,\phi_\nu(x, z). \quad (2)$$

Here ν is a discrete index of the transverse electric (TE) modes (discreteness arises due to the outgoing boundary conditions' see Refs. [21,22] for details), and $\beta_\nu^2(z)$ stands for the associated modal eigenvalue (formulation including the transverse magnetic (TM) modes whose polarization is perpendicular to TE modes goes along analogous lines). An appropriate normalization is imposed (based upon the so-called c product; see again Ref. [22]), such that

$$(\phi_\nu|\phi_{\nu'})_x = \langle \phi_\nu^*|\phi_{\nu'}\rangle_x = \delta_{\nu\nu'} \quad (\text{all } z). \quad (3)$$

Subsequently, one returns to Eq. (1), and expands $\Psi(x, z)$ in the z-adiabatic basis set as follows:

$$\Psi(x, z) = \sum_\nu C_\nu(z)\phi_\nu(x, z), \quad (4)$$

where

$$C_\nu(z) = (\phi_\nu|\Psi)_x. \quad (5)$$

[The usual adiabatic dynamical phase factor $e^{+i\int_0^z \beta_\nu(z')\,dz'}$ is implicitly embedded in the coefficients $C_\nu(z)$.] This results in a coupled-channel problem

$$\partial_{zz}\vec{C}(z) + \mathbb{A}(z)\,\partial_z\vec{C}(z) + \mathbb{B}(z)\vec{C}(z) = \vec{0}, \quad (6)$$

where by definition

$$A_{\nu\nu'}(z) = 2\,(\phi_\nu|\partial_z\phi_{\nu'})_x, \quad (7)$$

$$B_{\nu\nu'}(z) = (\phi_\nu|\partial_{zz}\phi_{\nu'})_x + \delta_{\nu\nu'}\,\beta_\nu^2(z). \quad (8)$$

The just outlined formulation converting Eq. (1) into an equivalent Eq. (6) is broadly used in molecular physics
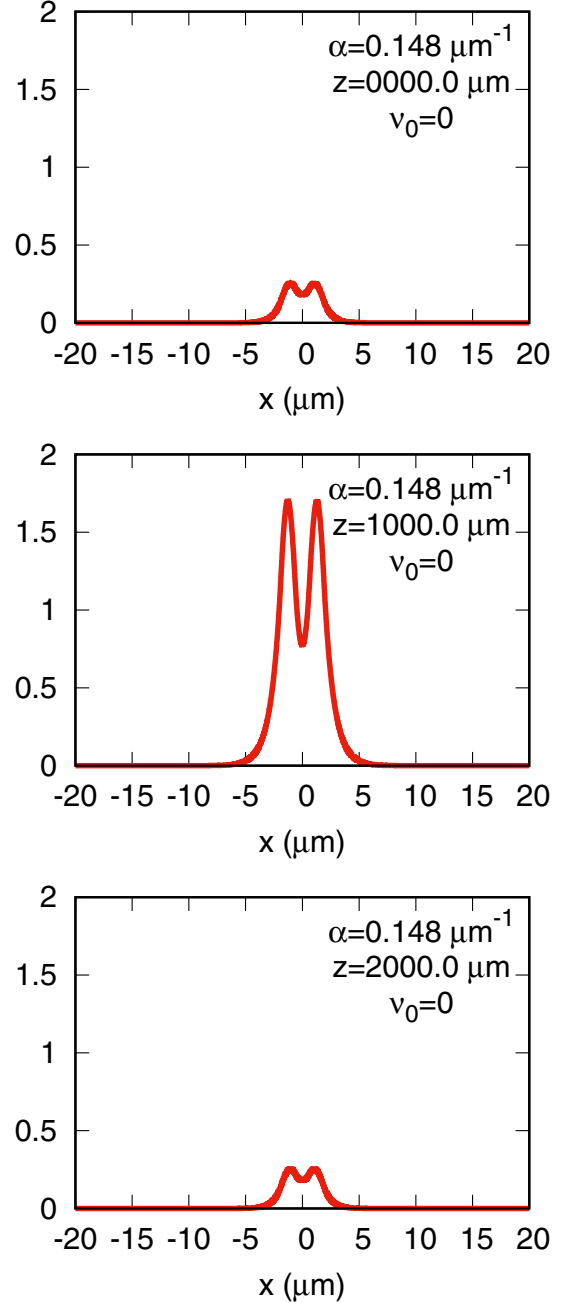

FIG. 2. Results for the straight case and $\alpha(1000\,\mu\text{m}) = 0.148\,\mu\text{m}^{-1}$. An initial population of the ground ($\nu_0 = 0$) guided mode. See the caption of Fig. 3 for an additional discussion.

and spectroscopy to study vibrational problems (see, e.g., Ref. [23] for details). Equation (6) needs to be solved for the unknowns $\vec{C}(z)$, while incorporating the appropriate scattering boundary conditions as specified below.

At the entry and at the exit from our WGs (i.e., for $z \to \pm\infty$), the index of refraction approaches its limiting z-independent profile $n(x) = n^*(x)$. Correspondingly, the z-adiabatic eigenproblem (2) yields z-independent solutions $\phi_\nu(x)$ and β_ν. The nonadiabatic couplings $(\phi_\nu|\partial_z\phi_{\nu'})_x$ and $(\phi_\nu|\partial_{zz}\phi_{\nu'})_x$ vanish; hence light propagates freely in each z-adiabatic mode $\phi_\nu(x)$ for $z \to \pm\infty$. Hence the only nontrivial

physics (scattering phenomena) takes place in that section of the WGs where $n(x, z)$ changes appreciably with z and where the $\mathcal{PT}$ symmetry is thus substantially broken. Accordingly, we impose the appropriate scattering boundary conditions on $\Psi(x, z \to \pm\infty)$, as detailed in Appendix A.

The just mentioned scattering boundary conditions provide immediately the corresponding boundary conditions for the sought particular solution $\vec{C}(z)$ of Eq. (6). The resulting boundary value problem (6) is solvable numerically on a grid by using any standard finite difference method.

III. OUR WAVEGUIDE SETUP

The corresponding WG setup is plotted schematically in Fig. 1 (for more details, see Refs. [12,13,24]). In all our numerical simulations, we use the WGs of width $W = 1.25 \ \mu$m and the mutual separation $D = 1.25 \ \mu$m, much as in Ref. [25]. The solid line of Fig. 1 marks a bent WG that is often used in conventional integrated optical circuits (having real index of refraction) to minimize loss of power. One has $x[\mu\text{m}](z) = R - \sqrt{R^2 - (z - 1000 \ \mu\text{m})^2}$, where $R = 3554 \ \mu$m is the radius of curvature measured from the center of the WGs.

IV. RESULTS AND DISCUSSION

A. Straight WGs

The considered refractive index profile is such that $n(x, z) = n^*(-x, z)$. A control parameter $\alpha(z)$ defines here the gain and loss strength as $\text{Im}[n] = \pm\alpha(z)/k$ with $k = \omega/c = 2\pi/\lambda$. At the entrance to the two coupled WGs and exit from them, the index of refraction is real, $\alpha(0) = 0 = \alpha(z = 2000 \ \mu\text{m})$. When light propagates inside the WG, $\alpha(z)$ increases gradually such that in the middle of the WGs it gets a maximal value of $\alpha(1000 \ \mu\text{m}) \equiv \alpha$. The value of $\alpha_{\text{EP}} = 0.150 \ \mu\text{m}^{-1}$ at which an EP is formed was found before in Ref. [12]. Note that the strength of the imaginary index of refraction is varied here along the propagation axis, whereas in Ref. [12] and in the first experiment [13] (which has demonstrated the concept of $\mathcal{PT}$ symmetry in optics) the index of refraction is held fixed along z.

Figures 2 and 3 present our results obtained for $\alpha = 0.148 \ \mu\text{m}^{-1}$. What is plotted in Figs. 2 and 3 is the resulting input-output signal as well as the signal in the middle of the WG ($z = 1000 \ \mu\text{m}$). One may observe that the profile at the output agrees exactly with the input profile; also the nodal structure is extremely well preserved. On the other hand, in the middle of the WG, the two plotted modal profiles possess a large magnitude and look almost identical. This is a consequence of proximity to the EP condition at $z = 1000 \ \mu\text{m}$. In passing we note that the just illustrated near singular behavior of the modes near the EP can be attributed to the previously reported stopping of light in the EP-adjusted WGs [25]. While the light slows down (stops) in the vicinity of (at) the EP, an additional light comes into the EP region from the entrance of the WGs, and thus the resulting light intensity is enhanced (increases) indefinitely.

Next, Figs. 4 and 5 depict the outcome obtained for the same WG setup as in Figs. 2 and 3 but for $\alpha = 0.14975 \ \mu\text{m}^{-1}$. Due to an extreme proximity to the EP in the middle of the WGs, the $z = 1000 \ \mu$m signal is strongly enhanced.
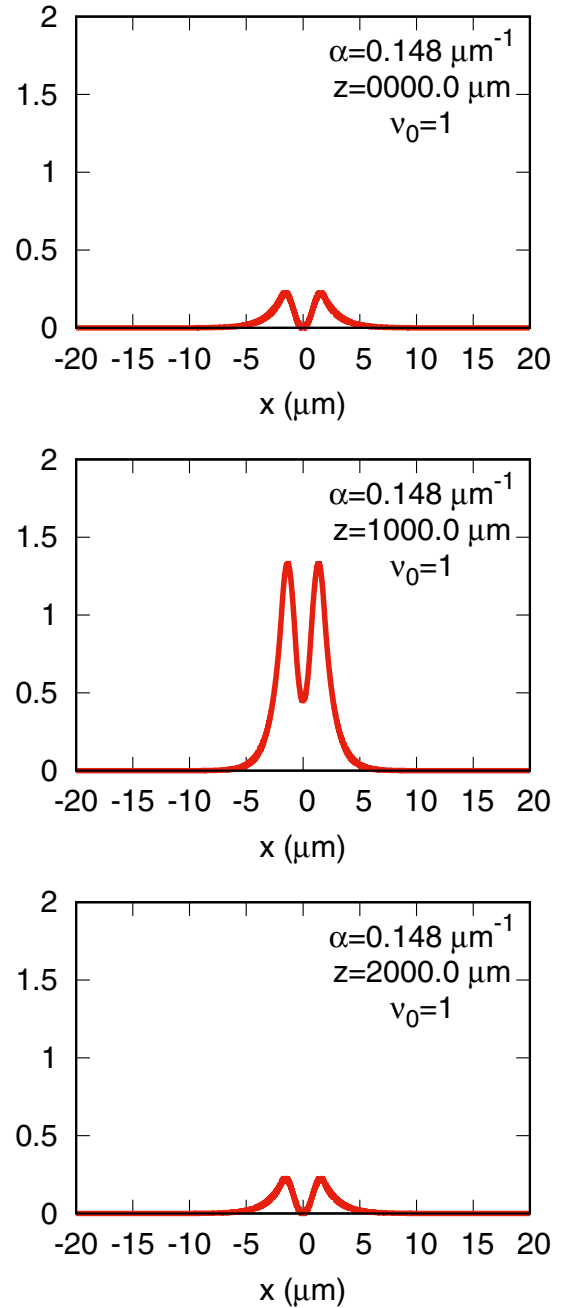

FIG. 3. Results for the straight case and $\alpha(1000 \ \mu\text{m}) = 0.148 \ \mu\text{m}^{-1}$. An initial population of the first excited ($\nu_0 = 1$) guided mode. Comparison with Fig. 2 shows that the $z = 1000 \ \mu$m profiles for $\nu_0 = 0$ and $\nu_0 = 1$ look almost identical; this is a consequence of proximity to the EP condition. On the other hand, the $z = 2000 \ \mu$m output profiles for $\nu_0 = 0$ and $\nu_0 = 1$ differ dramatically, and practically coincide with their input counterparts.

Moreover, a nontrivial scattering takes place, resulting in a pronounced reflection and affecting substantially also the transmitted profiles. Note that the nodal structure is still quite well preserved at the output, in spite of a substantial mixing between the two involved z-adiabatic modes.

Figure 6 compares the two above considered cases of $\alpha = 0.148 \ \mu\text{m}^{-1}$ and $\alpha = 0.14975 \ \mu\text{m}^{-1}$ by plotting the z derivative of the $\mathcal{PT}$-conserved charge $Q(z) =$
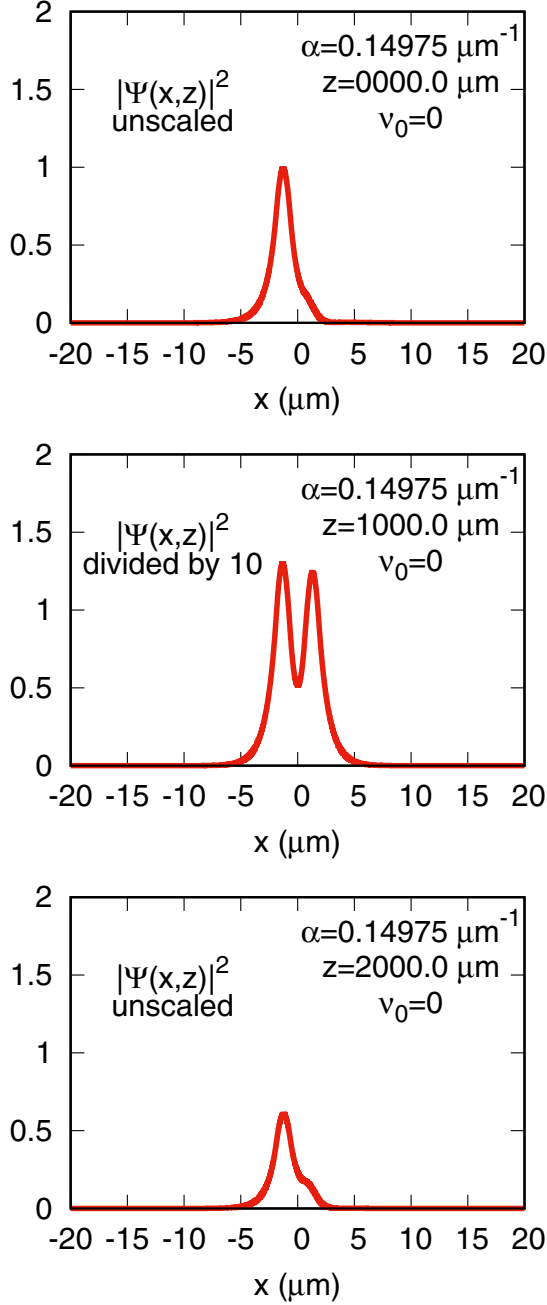
FIG. 4. The same setup as in Fig. 2, but now for $\alpha = 0.14975 \ \mu m^{-1}$, extremely close to an EP. Nontrivial scattering takes place here, including a pronounced reflection. Note that the nodal structure is still quite well preserved at the output, in spite of a substantial mixing between the two involved z-adiabatic modes.

$\int_{-\infty}^{+\infty} \Psi^*(-x, z) \, \Psi(+x, z) \, dx$. As a matter of fact, $\frac{d}{dz} Q(z) = 0$ if and only if the $\mathcal{PT}$ symmetry is preserved at a given location z [12]. An inspection of Fig. 6 reveals that the $\mathcal{PT}$ symmetry of the problem is strongly violated for $\alpha = 0.14975$ (even in the middle of the WGs); this is also associated with the nontrivial scattering phenomena reported above.

To the best of our knowledge, the above reported behavior of straight WGs has not been reported before. It follows then that, even for $\alpha = 0.148 \ \mu m^{-1}$ (i.e., quite close to
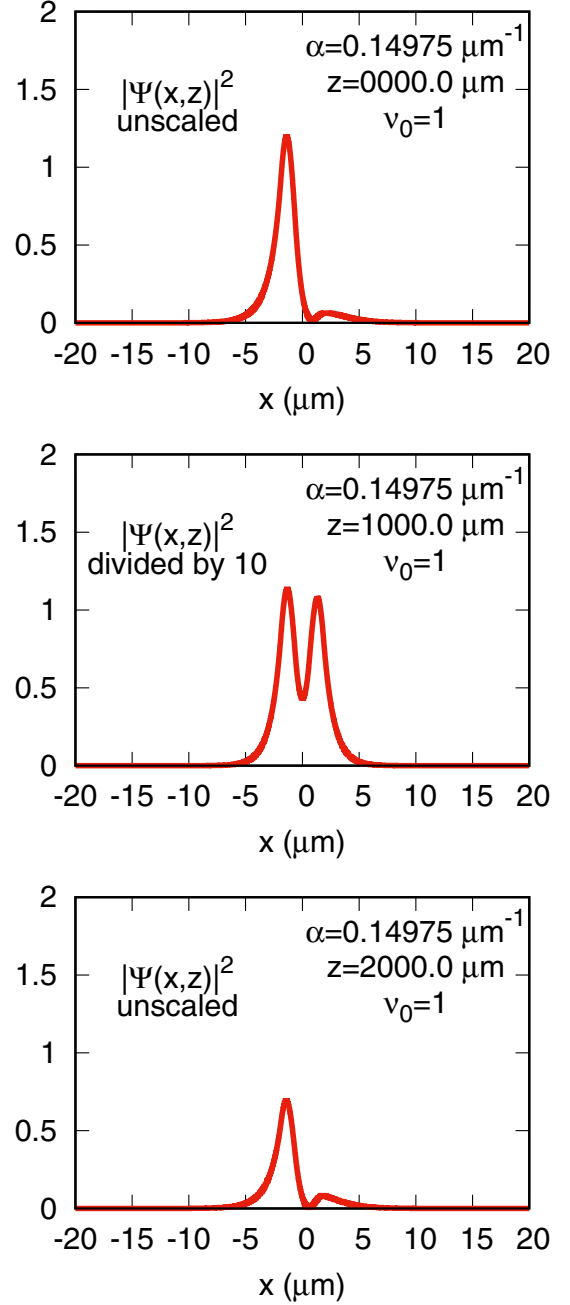
FIG. 5. The same setup as in Fig. 3, but now for $\alpha = 0.14975 \ \mu m^{-1}$, extremely close to an EP. See the caption of Fig. 4 for additional discussion.

$\alpha_{EP} = 0.150 \ \mu m^{-1}$), information can be transferred through our non-Hermitian straight WGs, while using the zero- and one-node modes as logical gates, in exactly the same manner as in Hermitian WGs. This holds in spite of passing near an EP (where the two mentioned modes are almost linearly dependent), and in spite of weakly breaking the $\mathcal{PT}$ symmetry when approaching the EP.

B. Slightly bent WGs

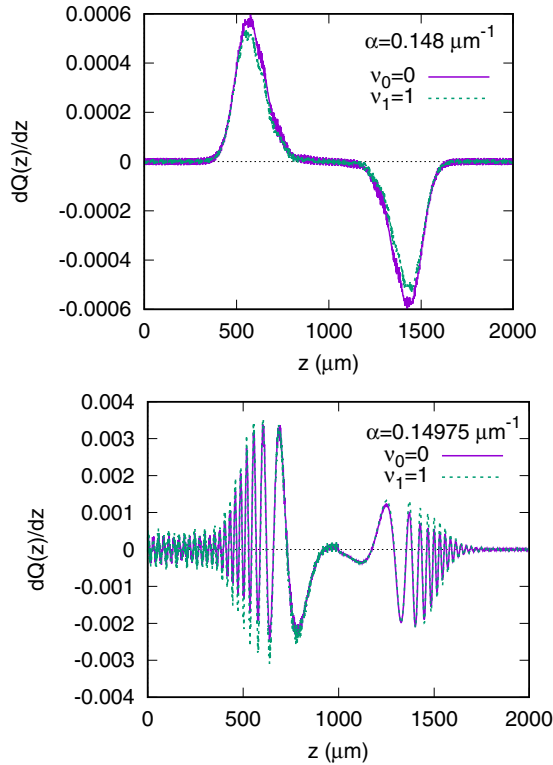In Fig. 7 we show another important result of the present article. Namely, by slightly bending the WGs of Figs. 2 and 3

FIG. 6. An examination of $\mathcal{PT}$ symmetry of the solution $\Psi(x,z)$ corresponding to Figs. 2 and 3 and Figs. 4 and 5. The z derivative of the $\mathcal{PT}$-conserved charge $Q(z) = \int_{-\infty}^{+\infty} \Psi^*(-x,z)\,\Psi(+x,z)\,dx$ vanishes if and only if the $\mathcal{PT}$ symmetry is preserved at a given location z [12].

we induce a dramatic enhancement or suppression of the output signal. We recall in this context that bending of the WGs is equivalent to adding to $n^2(x,z)$ an extra linear term [26,27]. In our case, this extra linear term is ζx with $\zeta = 2\,n_{\text{eff}}/R$. Here $n_{\text{eff}} = (2\pi)^{-1}\lambda\,\beta_{\text{EP}}$, and β_{EP} stands for the real propagation constant in the middle of the WGs. The quantity R is the already encountered radius of curvature measured from the center of the WGs.
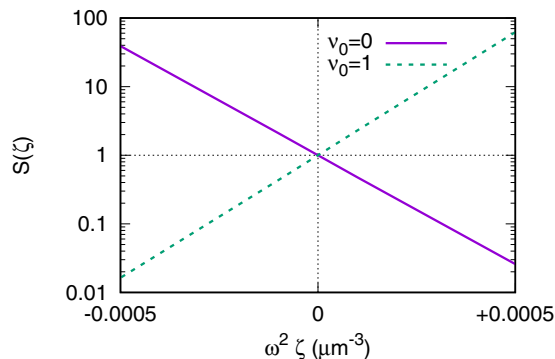

FIG. 7. The output amplitude $S(\zeta) = \int_{-\infty}^{+\infty} |\Psi(x,z = 2000\,\mu\text{m})|^2\,dx$ calculated for different values of the bending parameter ζ while holding $\alpha = 0.148\,\mu\text{m}^{-1}$. One observes that $S(\zeta)$ depends exponentially upon ζ, such that $S(\zeta) \sim e^{-\zeta/\omega}$ for $\nu_0 = 0$ and $S(\zeta) \sim e^{+\zeta/\omega}$ for $\nu_0 = 1$.

Most importantly, Fig. 7 demonstrates that the just described slight bending affects very strongly the resulting output signals. Namely, while both the shape and the nodal structure remain unaffected, the magnitude is enhanced or suppressed depending upon the direction of the bending. The closer are the WG parameters adjusted to the EP condition, the larger is the sensitivity of the output results with respect to bending.

The observed strong sensitivity of the output information with respect to bending can be understood as follows. Recall again that bending of the WGs is analogous to adding an extra linear term (i.e., application of a static field) along the x direction, perpendicular to the propagation direction z [26,27]. In the Hermitian case, when the two WGs (equivalent to two potential wells in quantum mechanics) are sufficiently far apart, such a static field mixes the two nearly degenerate field modes $\nu_0 = 0$ and $\nu_0 = 1$, and forces each of the modes to be localized inside just a single WG branch (i.e., in a single potential well for an equivalent quantum mechanical problem) [28,29]. The propagation constants remain real valued. In our non-Hermitian case, the mixing of the two involved modes breaks the $\mathcal{PT}$ symmetry of the two coupled WGs. The corresponding propagation constants become then slightly complex, and therefore enhance or suppress the signal accordingly, exactly as plotted in Fig. 7.

The above pursued discussion of bent WGs can be supported by the following explicit mathematical arguments. As pointed out already, bending the WGs means perturbing the z-adiabatic modes by action of an extra linear term ζx (with $\zeta \sim 1/R$) [26,27]. Assume first that the WG parameters are chosen to be far from the EP. The standard perturbation method shows then that the modal eigenvalues, $\beta_\nu(z)$, are slightly changed by bending into

$$\beta_\nu^\zeta(z) = \beta_\nu(z) + \zeta\,(\phi_\nu|x|\phi_\nu)_x + O(\zeta^2)\,. \qquad (9)$$

Here the modal function $\phi_\nu(x,z)$ is almost real valued far from the EP. Thus the correction term $(\phi_\nu|x|\phi_\nu)_x = \langle\phi_\nu^*|x|\phi_\nu\rangle_x$ is almost real valued also. Assume now that the WG parameters are chosen to be close to (or even at) the EP. In that case, one needs use a nonstandard perturbation theory (resulting in the so-called Puiseux series expansion; see Ref. [22]), which gives

$$\beta_\pm^\zeta(z) = \beta_{\text{EP}} \pm \sqrt{(\zeta_{\text{EP}} - \zeta)(\phi_{\text{EP}}|x|\phi_{\text{EP}})_x} + O(\zeta)$$
$$= \beta_{\text{EP}} \pm i\sqrt{\zeta\,(\phi_{\text{EP}}|x|\phi_{\text{EP}})_x} + O(\zeta), \qquad (10)$$

where β_{EP} is real, and $\zeta_{\text{EP}} = 0$ is a branch point where a transition from real to complex modal eigenvalues is obtained. [The quantity $(\phi_{\text{EP}}|x|\phi_{\text{EP}})_x$ is generally complex, since the modal function $\phi_{\text{EP}}(x,z)$ is complex valued and self-orthogonal.] Comparison between the two cases (9) and (10) shows immediately that the effect of bending is by far much larger in the EP situation, first because $\sqrt{\zeta} \gg \zeta$ (ζ small), and second because the resulting perturbation correction is complex in Eq. (10). This leads to the corresponding enhancement or suppression of the propagated signal, as described by the associated exponential term $e^{+i\int_0^z \beta_\nu^\zeta(z')\,dz'}$. Indeed, the mentioned term $e^{+i\int_0^z \beta_\nu^\zeta(z')\,dz'}$ diverges to $+\infty$ for increasing z when $\text{Im}\beta_\nu^\zeta(z) < 0$, and falls off to zero when $\text{Im}\beta_\nu^\zeta(z) > 0$.

V. CONCLUDING REMARKS

We have studied propagation of light in a pair of non-Hermitian WGs whose parameters are close to an EP. We have shown that information can be transferred through such non-Hermitian straight WGs, while using the zero- and one-node modes as logical gates. The signal is transferred here exactly in the same manner as in the usual Hermitian WGs, in spite of passing near an EP where the two mentioned modes are almost linearly dependent, and in spite of weakly breaking the $\mathcal{PT}$ symmetry when approaching the EP.

Furthermore, we have investigated sensitivity of our non-Hermitian WGs with respect to bending. It was shown that a slight bending (which might not be avoided in experiments) does not change much the nodal structure of the transferred optical signal. However, the transferred information is exponentially sensitive to the strength of bending, and this has a dramatic amplification or suppression effect on the output. If so, then the transfer of optical information in our proposed WGs setup is protected from tapping light into another externally attached WG [9,10], since this requires a significant bending (that allows the leakage of the transmitted information). A similar argument is expected to hold also in the case of any other disturbance (like, e.g., a point defect) which one may create as to extract the transmitted information out of the WGs.

In summary, the non-Hermitian WGs considered in the present paper behave qualitatively differently than ordinary Hermitian or $\mathcal{PT}$-symmetric WGs without an EP. The just presented findings can be demonstrated experimentally by using, e.g., the setup described in Ref. [13], and open the ability of secure transfer of an uncoded information through optical WGs. Our results are further illustrated by additional plots given in Appendix B.

ACKNOWLEDGMENTS

APPENDIX A: TRANSMISSION AND REFLECTION OF LIGHT IN OPTICAL WAVEGUIDES WITH A COMPLEX REFRACTION INDEX

1. Basic scattering theory for complex $n(x, z)$

Propagation of light in our studied optical WGs is described by the wave equation (1) of the main text. Here $n(x, z)$ stands for a given prescribed index of refraction, such that

$$\lim_{z \to \pm\infty} n(x, z) = \tilde{n}(x). \tag{A1}$$

The solution $\Psi(x, z)$ of Eq. (1) is required to be bounded for all (x, z) and vanishing for $x \to \pm\infty$. Moreover, $\Psi(x, z)$ must satisfy appropriate scattering boundary conditions imposed at $z \to \pm\infty$, as detailed below.

In the asymptotic region of $z \to \pm\infty$, Eq. (1) reduces to

$$(\partial_{xx} + \omega^2 \tilde{n}^2(x) + \partial_{zz}) \Psi(x, z) = 0. \tag{A2}$$

The problem thus becomes separable in coordinates x and z. Stated mathematically, our sought solution $\Psi(x, z)$ can be for $z \to \pm\infty$ expressed in the form

$$\Psi(x, z \to \pm\infty)$$
$$= \sum_\nu A_\nu^\pm \phi_\nu(x) \frac{e^{+i\beta_\nu z}}{\sqrt{2\beta_\nu}} + B_\nu^\pm \phi_\nu(x) \frac{e^{-i\beta_\nu z}}{\sqrt{2\beta_\nu}}, \tag{A3}$$

with the involved symbols explained as follows. Entities $\phi_\nu(x)$ and β_ν are defined by an eigenvalue problem

$$(\partial_{xx} + \omega^2 \tilde{n}^2(x)) \phi_\nu(x) = \beta_\nu^2 \phi_\nu(x),$$
$$\phi_\nu(x \to \pm\infty) = 0. \tag{A4}$$

Here ν stands for a discrete label of the eigenstates. We restrict our considerations to guided modes only ($\beta_\nu^2 > 0$). Entities $A_\nu^\pm$ and $B_\nu^\pm$ represent as yet arbitrary coefficients.

Considerations of the previous paragraph enable us to impose now the scattering boundary conditions on $\Psi(x, z \to \pm\infty)$. Namely, we require having

$$\Psi(x, z \to -\infty)$$
$$= \phi_{\nu_0}(x) \frac{e^{+i\beta_{\nu_0} z}}{\sqrt{2\beta_{\nu_0}}} + \sum_\nu R_\nu \phi_\nu(x) \frac{e^{-i\beta_\nu z}}{\sqrt{2\beta_\nu}} \tag{A5}$$

and

$$\Psi(x, z \to +\infty) = \sum_\nu T_\nu \phi_\nu(x) \frac{e^{+i\beta_\nu z}}{\sqrt{2\beta_\nu}}, \tag{A6}$$

where ν_0 is prescribed, and T_ν and R_ν are as yet unknown coefficients to be found. The physical meaning of the just imposed boundary conditions is the following: The term

$$\phi_{\nu_0}(x) \frac{e^{+i\beta_{\nu_0} z}}{\sqrt{2\beta_{\nu_0}}} \tag{A7}$$

represents an incoming wave sent into the waveguide. We assume that the incoming signal populates only a single mode ν_0. The term

$$\sum_\nu T_\nu \phi_\nu(x) \frac{e^{+i\beta_\nu z}}{\sqrt{2\beta_\nu}} \tag{A8}$$

represents the transmitted wave coming out of the waveguide in the forward direction. The T_ν's stand for the associated transmission coefficients. The term

$$\sum_\nu R_\nu \phi_\nu(x) \frac{e^{-i\beta_\nu z}}{\sqrt{2\beta_\nu}} \tag{A9}$$

represents the reflected wave coming out of the waveguide in the backward direction. The R_ν's stand for the associated reflection coefficients. One can see that we are dealing here with multichannel scattering phenomena analogous to those of quantum mechanics.

Our task is now to construct explicitly the solution $\Psi(x, z)$ of the wave equation (1) supplemented by the boundary conditions (A5) and (A6). This can be accomplished by taking

advantage of an ingenuous trick of Ref. [31]: One resolves first a collection of auxiliary problems

$$(\partial_{xx} + \omega^2 n^2(x,z) + \partial_{zz}) \Psi^{(\nu)}(x,z) = 0, \qquad \text{(A10)}$$

$$\Psi^{(\nu)}(x, z \to +\infty) = \phi_\nu(x) \frac{e^{+i\beta_\nu z}}{\sqrt{2\beta_\nu}}. \qquad \text{(A11)}$$

The solution $\Psi^{(\nu)}(x,z)$ of Eqs. (A10) and (A11) is well defined and unique. Its asymptotic behavior at $z \to -\infty$ is described by the formula

$$\Psi^{(\nu)}(x, z \to -\infty)$$
$$= \sum_{\nu'} F_{\nu'\nu} \phi_{\nu'}(x) \frac{e^{+i\beta_{\nu'}z}}{\sqrt{2\beta_{\nu'}}} + G_{\nu'\nu} \phi_{\nu'}(x) \frac{e^{-i\beta_{\nu'}z}}{\sqrt{2\beta_{\nu'}}}, \quad \text{(A12)}$$

where $\mathbb{F} = [F_{\nu'\nu}]$ and $\mathbb{G} = [G_{\nu'\nu}]$ are certain well-defined matrices. Subsequently, one constructs the desired solution $\Psi(x,z)$ of our problem (1) and Eqs. (A5) and (A6) by taking a linear combination

$$\Psi(x,z) = \sum_\nu c_\nu \Psi^{(\nu)}(x,z). \qquad \text{(A13)}$$

The pertinent coefficients $\mathbf{c} = [c_\nu]$ are fixed in such a way as to fulfill boundary condition (A5), meaning that

$$\mathbb{F}\,\mathbf{c} = \mathbf{f}^{(\nu_0)}, \qquad \text{(A14)}$$

where the column vector $\mathbf{f}^{(\nu_0)}$ possesses zero components everywhere except for the ν_0th component (which equals unity). Correspondingly

$$\mathbf{c} = \mathbb{F}^{-1}\mathbf{f}^{(\nu_0)}, \qquad \text{(A15)}$$

and this yields in turn

$$\mathbf{t} \equiv [T_\nu] = \mathbf{c}, \qquad \text{(A16)}$$

$$\mathbf{r} \equiv [R_\nu] = \mathbb{G}\,\mathbf{c} = \mathbb{G}\,\mathbb{F}^{-1}\mathbf{f}^{(\nu_0)}. \qquad \text{(A17)}$$

The desired solution $\Psi(x,z)$ of our problem (1) and Eqs. (A5) and (A6) has thus just been built.

2. Probability conservation in non-Hermitian scattering: The case of general $n(x,z)$

Let us return to Eq. (1). Assume that the index of refraction $n(x,z)$ is generally complex valued. If so, then the studied problem is non-Hermitian, and the appropriate non-Hermitian probability conservation law needs to be established by using the formalism of the mutually associated left and right solutions $\Psi_L(x,z)$ and $\Psi_R(x,z)$ of Eq. (1). A general account of the left-right formalism is given, e.g., in Ref. [22].

The entities $\Psi_L(x,z)$ and $\Psi_R(x,z)$ are defined by the following boundary value problems:

$$(\partial_{xx} + \omega^2 n^2(x,z) + \partial_{zz})\Psi_R(x,z) = 0, \qquad \text{(A18)}$$

$$(\partial_{xx} + \omega^2 n^2(x,z) + \partial_{zz})\Psi_L(x,z) = 0, \qquad \text{(A19)}$$

where

$$\Psi_R(x, z \to -\infty)$$
$$= \phi_{\nu_0}(x) \frac{e^{+i\beta_{\nu_0}z}}{\sqrt{2\beta_{\nu_0}}} + \sum_\nu R_\nu^{(R)} \phi_\nu(x) \frac{e^{-i\beta_\nu z}}{\sqrt{2\beta_\nu}}, \quad \text{(A20)}$$

$$\Psi_R(x, z \to +\infty) = \sum_\nu T_\nu^{(R)} \phi_\nu(x) \frac{e^{+i\beta_\nu z}}{\sqrt{2\beta_\nu}}, \qquad \text{(A21)}$$

and

$$\Psi_L(x, z \to -\infty)$$
$$= \phi_{\nu_0}(x) \frac{e^{-i\beta_{\nu_0}z}}{\sqrt{2\beta_{\nu_0}}} + \sum_\nu R_\nu^{(L)} \phi_\nu(x) \frac{e^{+i\beta_\nu z}}{\sqrt{2\beta_\nu}}, \quad \text{(A22)}$$

$$\Psi_L(x, z \to +\infty) = \sum_\nu T_\nu^{(L)} \phi_\nu(x) \frac{e^{-i\beta_\nu z}}{\sqrt{2\beta_\nu}}. \qquad \text{(A23)}$$

Note that, for real-valued $n(x,z)$, we have $\Psi_L(x,z) = \Psi_R^*(x,z)$. On the other hand, for generally complex $n(x,z)$, the entity $\Psi_L(x,z)$ is generally different from $\Psi_R^*(x,z)$.

Define the corresponding Wronskian

$$W(z)$$
$$= \int_{-\infty}^{+\infty} dx\, \Psi_L(x,z) i\partial_z \Psi_R(x,z) - \Psi_R(x,z) i\partial_z \Psi_L(x,z).$$
$$\text{(A24)}$$

This is a generally complex-valued entity. Importantly, $W(z)$ is actually z independent, since

$$\partial_z W(z)$$
$$= \int_{-\infty}^{+\infty} dx\, \Psi_L(x,z)\, i\, \partial_{zz} \Psi_R(x,z) - \Psi_R(x,z)\, i\, \partial_{zz} \Psi_L(x,z)$$
$$= \int_{-\infty}^{+\infty} dx$$
$$\times \Psi_L(x,z)\, i\, (-\partial_{xx} - \omega^2 n^2(x,z))\, \Psi_R(x,z)$$
$$- \Psi_R(x,z)\, i\, (-\partial_{xx} - \omega^2 n^2(x,z))\, \Psi_L(x,z)$$
$$= (-i)\int_{-\infty}^{+\infty} dx$$
$$\times \Psi_L(x,z)\, \partial_{xx} \Psi_R(x,z) - \Psi_R(x,z)\, \partial_{xx} \Psi_L(x,z) = 0,$$
$$\text{(A25)}$$

as follows using integration by parts. Thus $W(z)$ is an entity which remains constant along the z direction. In passing we note that our just given proof of $\partial_z W(z) = 0$ has not exploited at all any boundary conditions imposed on $\Psi_{R,L}(x,z)$.

In practice, we calculate $\Psi_{R,L}(x,z)$ using the method of adiabatic expansion [see Eq. (4) of the main text], such that

$$\Psi_{R,L}(x,z) = \sum_\nu C_\nu^{R,L}(z)\phi_\nu(x,z). \qquad \text{(A26)}$$

Here $\phi_\nu(x,z)$ are generally complex-valued entities defined by an eigenproblem

$$(\partial_{xx} + \omega^2 n^2(x,z))\,\phi_\nu(x,z) = \beta_\nu^2(z)\,\phi_\nu(x,z),$$
$$\phi_\nu(x \to \pm\infty) = 0 \qquad \text{(A27)}$$

[see Eq. (2) of the main text and the accompanying discussion]. Recall that the ϕ_ν's are orthonormalized with respect to the c product [22],

$$(\phi_\nu | \phi_{\nu'})_x = \int_{-\infty}^{+\infty} \phi_\nu(x,z)(\phi_{\nu'}(x,z)dx = \delta_{\nu\nu'}. \qquad \text{(A28)}$$
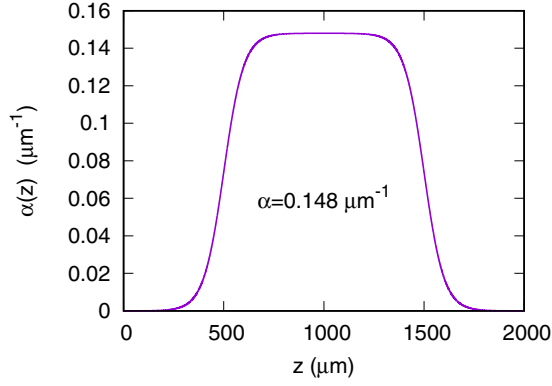
FIG. 8. Function $\alpha(z)$ determining the imaginary part of the refraction index, such that $\mathrm{Im}\,n(x, z) = \alpha(z)/k$ where $k = 2\pi/\lambda$. Note that $\alpha(z)$ is almost constant around $z = 1000\ \mu$m where the EP is approached.

After plugging Eq. (A26) into Eq. (A24) one finds that

$$
\begin{aligned}
W(z) &= \sum_\nu \left(C_\nu^L(z) i \partial_z C_\nu^R(z) - C_\nu^R(z) i \partial_z C_\nu^L(z) \right) \\
&\quad + \sum_{\nu\nu'} \\
&\quad \times \left(C_\nu^L(z) C_{\nu'}^R(z) i\,(\phi_\nu | \partial_z \phi_{\nu'})_x - C_\nu^R(z) C_{\nu'}^L(z) i\,(\phi_\nu | \partial_z \phi_{\nu'})_x \right) \\
&= \sum_\nu \left(C_\nu^L(z) i \partial_z C_\nu^R(z) - C_\nu^R(z) i \partial_z C_\nu^L(z) \right) \\
&\quad + \sum_{\nu\nu'} C_\nu^L(z) C_{\nu'}^R(z) 2i\,(\phi_\nu | \partial_z \phi_{\nu'})_x .
\end{aligned}
\tag{A29}
$$

Formula (A29) is suitable for a practical numerical calculation of $W(z)$. One may evaluate $W(z)$ along the z direction, and check whether it remains constant. This is a strong test of our numerical calculations.

The above discussed Wronskian provides a key leading towards the sought non-Hermitian law of probability conservation. Namely, direct calculation yields

$$
W(z \to +\infty) = -\sum_\nu T_\nu^{(L)} T_\nu^{(R)}
\tag{A30}
$$

and

$$
W(z \to -\infty) = -1 + \sum_\nu R_\nu^{(L)} R_\nu^{(R)} .
\tag{A31}
$$

There are some extra z-dependent oscillating terms appearing in $W(z \to -\infty)$, yet these are granted to vanish since $W(z)$ has been demonstrated to be z independent. Thus altogether

$$
\sum_\nu T_\nu^{(L)} T_\nu^{(R)} + \sum_\nu R_\nu^{(L)} R_\nu^{(R)} = 1,
\tag{A32}
$$

which is valid in the most general non-Hermitian case. This is the sought law of non-Hermitian probability conservation.
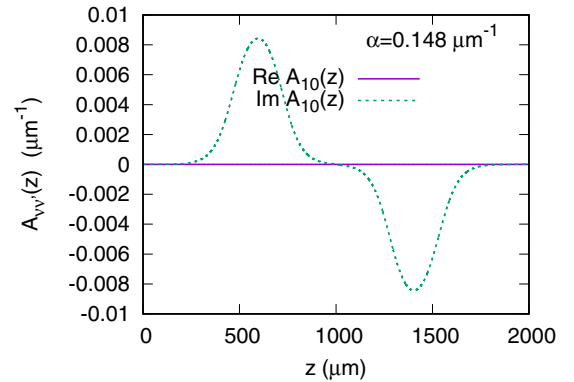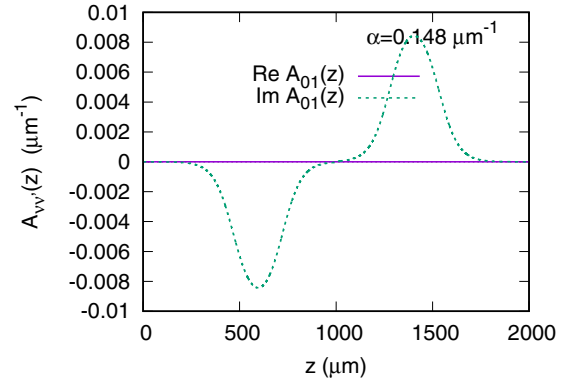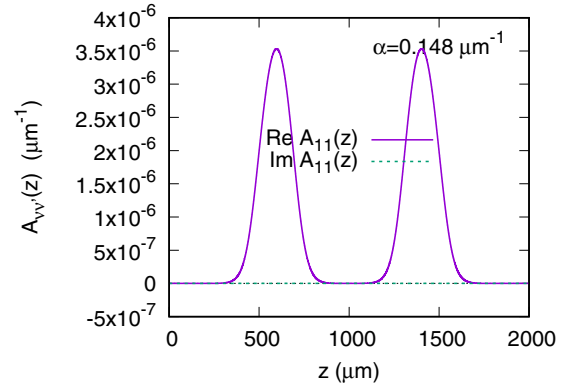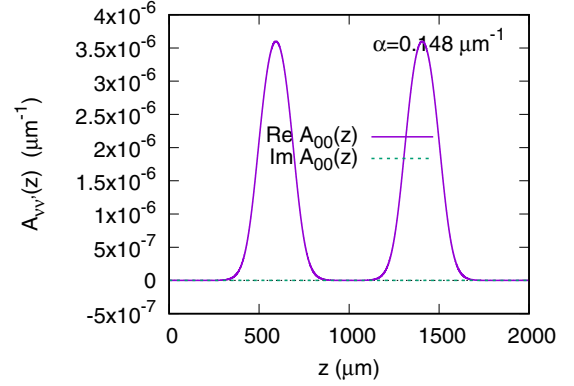

FIG. 9. The matrix $\mathbb{A}(z)$ defined by Eq. (7) of the main text. Results obtained for the case of straight WGs and $\alpha(1000\,\mu\text{m}) = 0.148\,\mu\text{m}^{-1}$.
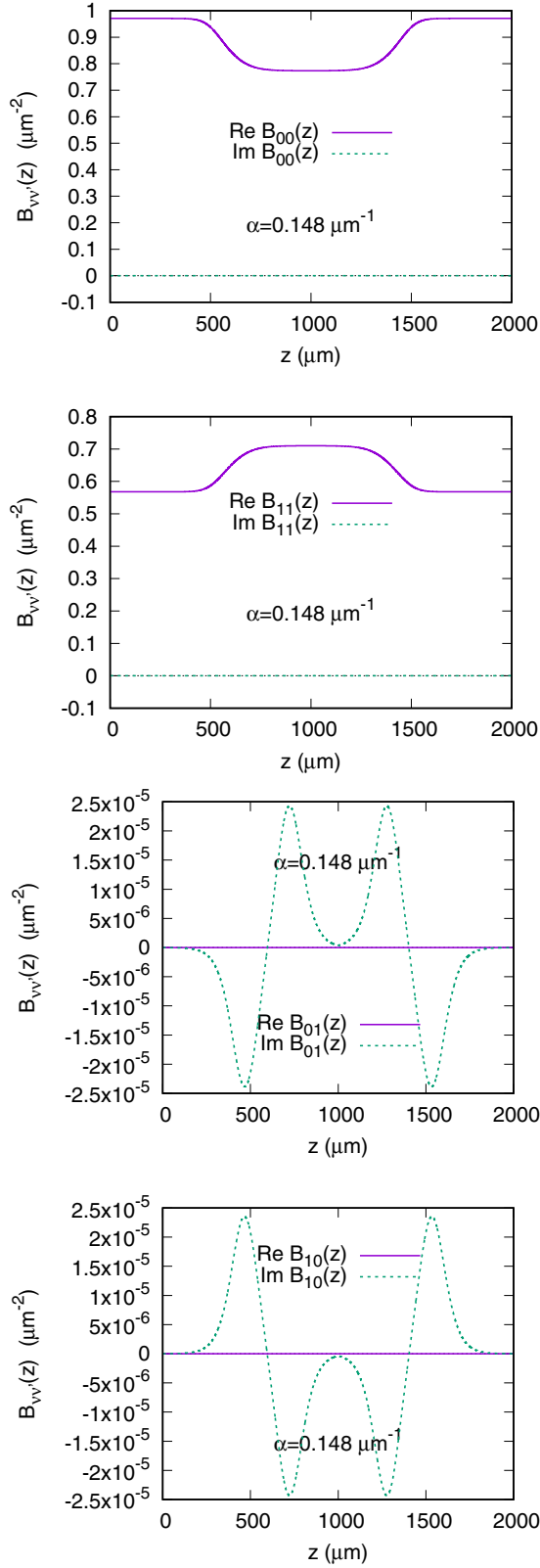
FIG. 10. The matrix $\mathbb{B}(z)$ defined by Eq. (8) of the main text. Results obtained for the case of straight WGs and $\alpha(1000\,\mu\mathrm{m}) = 0.148\,\mu\mathrm{m}^{-1}$.
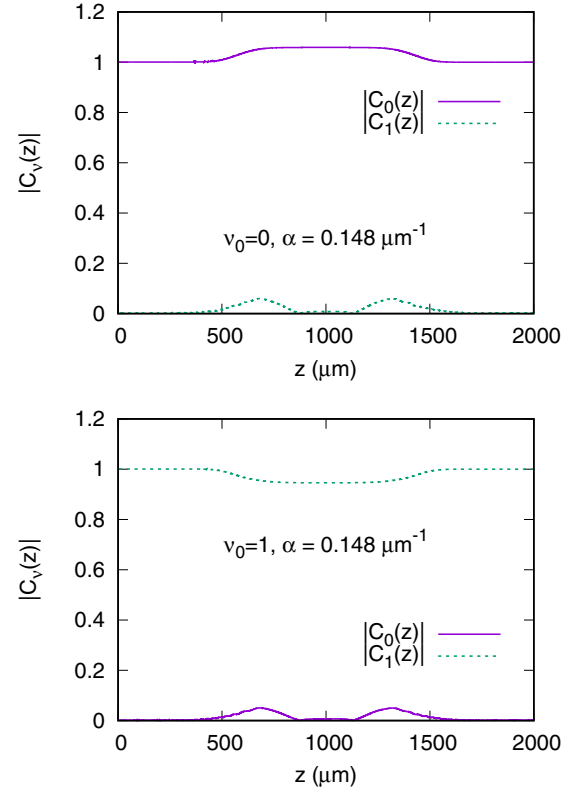

FIG. 11. The coefficients $C_\nu(z)$ corresponding to the adiabatic basis set expansion (4) of the main text and to the solution plotted in Figs. 2 and 3 of the main text. One can see that, for $\alpha(1000\,\mu m) = 0.148\,\mu m^{-1}$, the mixing between the $\nu = 0$ and $\nu = 1$ z-adiabatic modes is rather small, in spite of proximity of the studied system to the EP ($\alpha_{\mathrm{EP}} = 0.150\,\mu m^{-1}$).

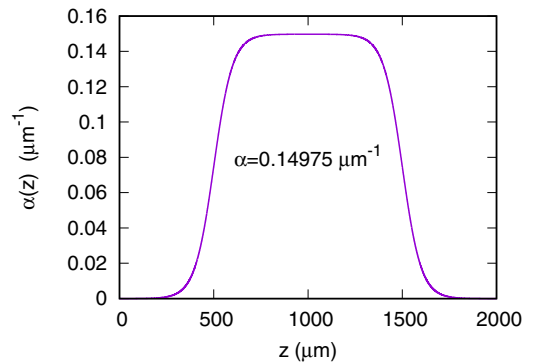Equation (A32) is very useful also for checking the accuracy of our numerical calculations.

FIG. 12. The function $\alpha(z)$ determining the imaginary part of the refraction index, such that $\mathrm{Im}\,n(x, z) = \alpha(z)/k$ where $k = 2\pi/\lambda$. Note that $\alpha(z)$ is almost constant around $z = 1000\,\mu m$ where the EP is approached.

FIG. 13. The matrix $\mathbb{A}(z)$ defined by Eq. (7) of the main text. Results obtained for the case of straight WGs and $\alpha(1000\,\mu\mathrm{m}) = 0.14975\,\mu\mathrm{m}^{-1}$.
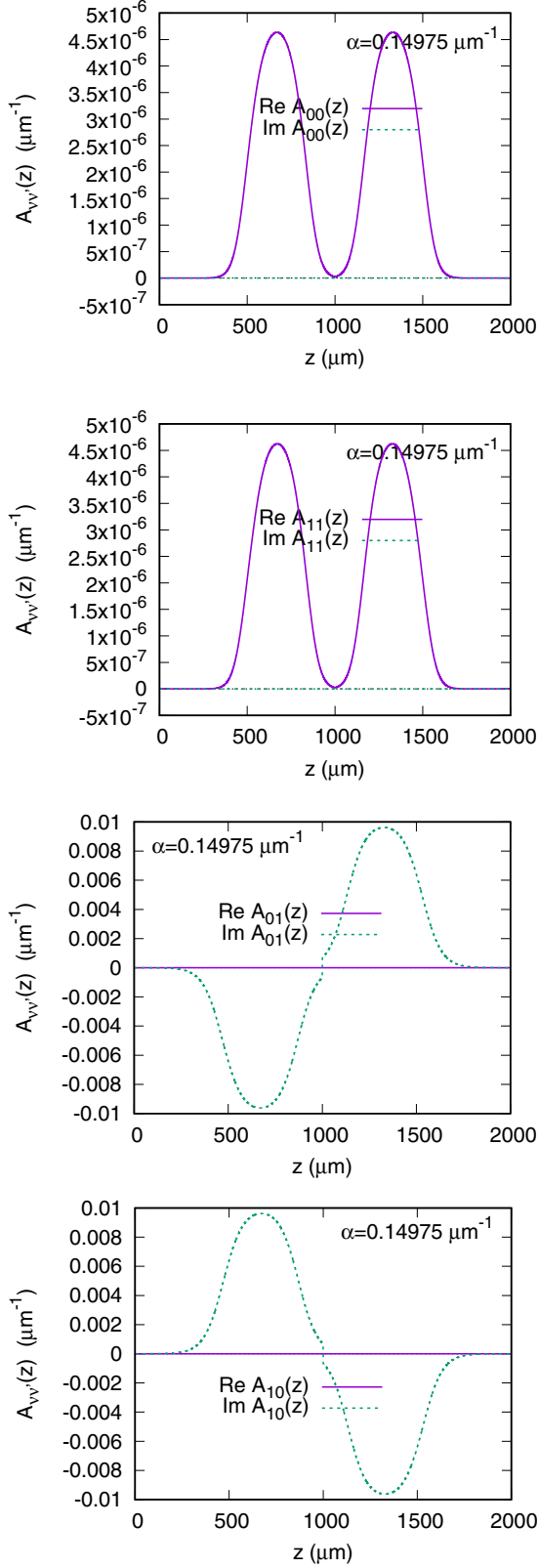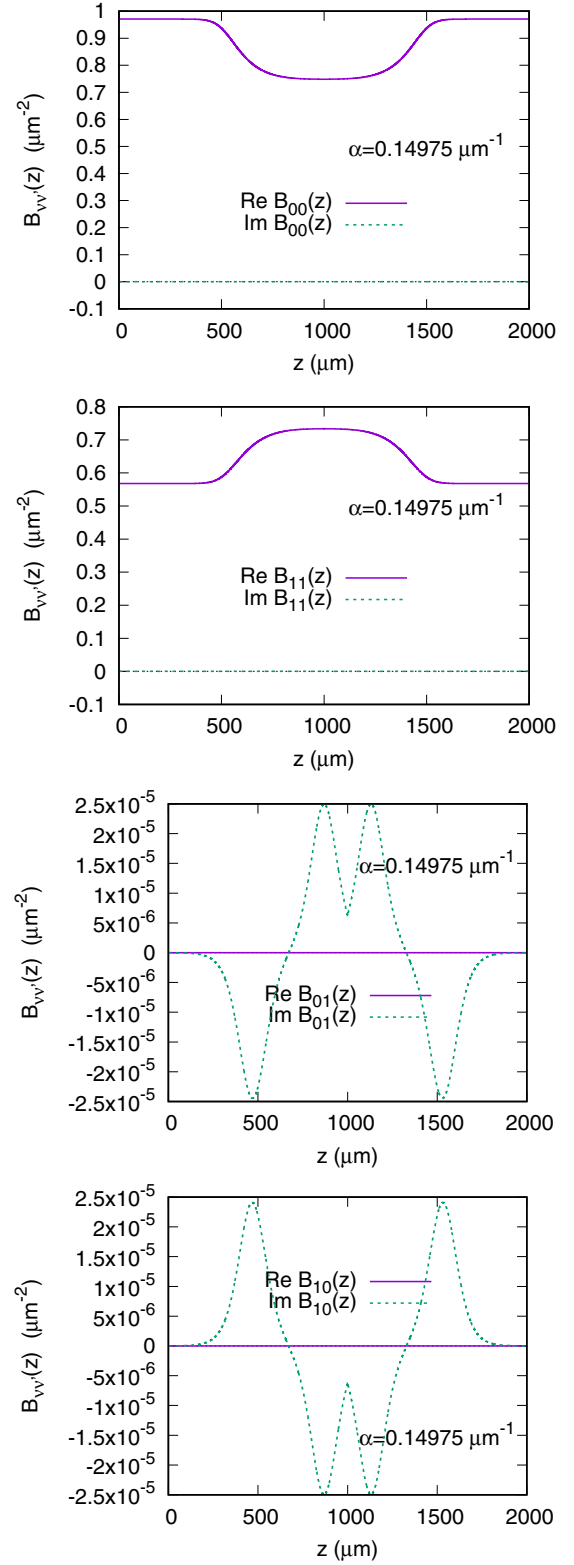

FIG. 14. The matrix $\mathbb{B}(z)$ defined by Eq. (8) of the main text. Results obtained for the case of straight WGs and $\alpha(1000\,\mu\mathrm{m}) = 0.14975\,\mu\mathrm{m}^{-1}$.
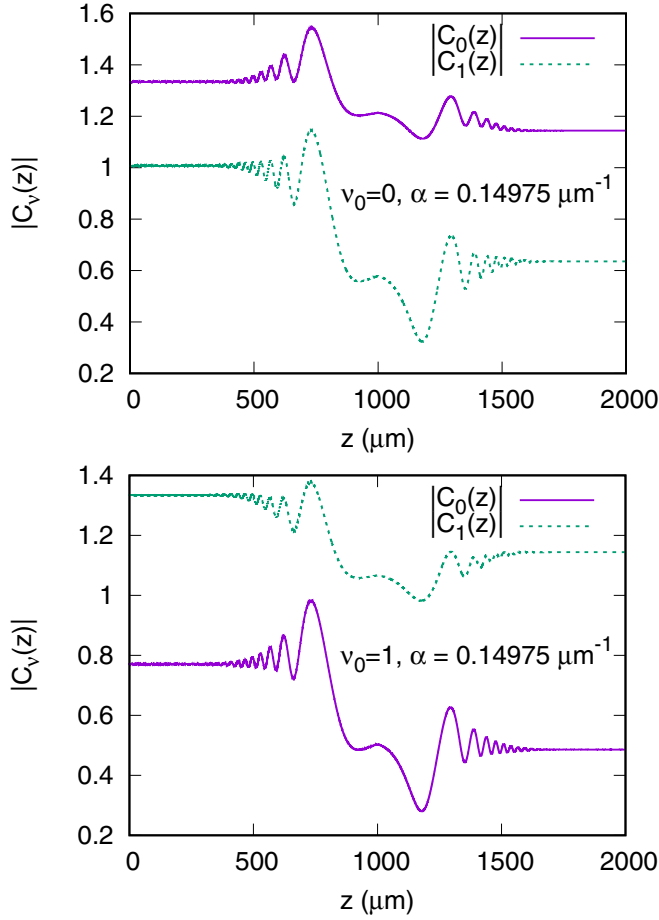
FIG. 15. The coefficients $C_\nu(z)$ corresponding to the adiabatic basis set expansion (4) of the main text and to the solution plotted in Figs. 4 and 5 of the main text. One can see that, for $\alpha(1000\,\mu\text{m}) = 0.14975\,\mu\text{m}^{-1}$, the mixing between the $\nu = 0$ and $\nu = 1$ z-adiabatic modes becomes very substantial due to an extremely close proximity of the studied system to the EP ($\alpha_{\text{EP}} = 0.150\,\mu\text{m}^{-1}$).

3. Probability conservation in non-Hermitian scattering: The case of $n(+x, z) = n^*(-x, z)$

From now on, let us consider a more special arrangement when $n(x, z)$ is complex valued but possesses the property

$$n^*(-x, z) = n(x, z), \tag{A33}$$

much as in Fig. 1 of the main text. Validity of Eq. (A33) is a necessary but *not* sufficient condition for having $\mathcal{PT}$ symmetry (real modal eigenvalues). A moment of reflection reveals that Eq. (A33) implies having

$$\Psi_L(x, z) = \Psi_R^*(-x, z), \tag{A34}$$

and

$$T_\nu^{(L)} = T_\nu^{(R)*}\wp_\nu, \quad R_\nu^{(L)} = R_\nu^{(R)*}\wp_\nu, \tag{A35}$$

where $\wp_\nu$ stands for parity of the mode $\phi_\nu(x)$, such that $\phi_\nu(-x) = \wp_\nu \phi_\nu(x)$. In particular, $\wp_0 = +1$ and $\wp_1 = -1$. The
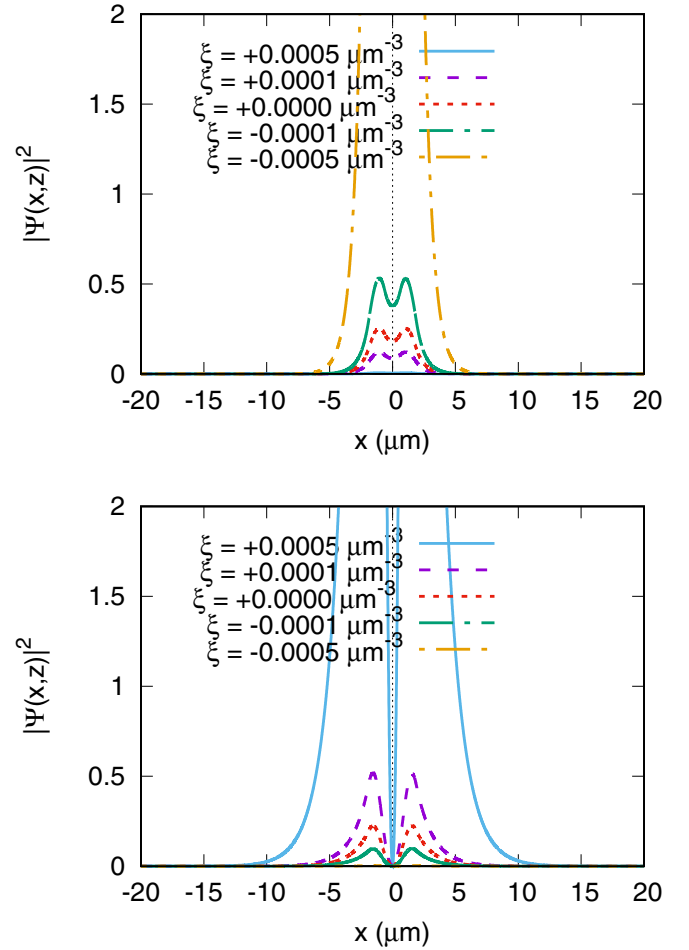

FIG. 16. This plot complements Fig. 7 of the main text and shows the effect of bending on the output signal for the case of $\alpha = 0.148\,\mu\text{m}^{-1}$. The upper panel corresponds to $\nu_0 = 0$, the lower panel to $\nu_0 = 1$. The strength of the bending (both magnitude and orientation) is characterized by the parameter $\xi = \omega^2\zeta$ as explained in the main text. Whenever the $\nu_0 = 0$ signal is enhanced, the $\nu_0 = 1$ signal is correspondingly suppressed, and vice versa.

conservation law (A32) is now converted into

$$\sum_\nu \wp_\nu \left|T_\nu^{(R)}\right|^2 + \sum_\nu \wp_\nu \left|R_\nu^{(R)}\right|^2 = 1. \tag{A36}$$

Moreover, the Wronskian (A24) becomes equal to

$$\begin{aligned} W(z) = \int_{-\infty}^{+\infty} dx \\ \times \Psi_R^*(-x, z)i\partial_z \Psi_R(x, z) \\ -\Psi_R(x, z)i\partial_z \Psi_R^*(-x, z). \end{aligned} \tag{A37}$$

This z-independent quantity is manifestly real valued.

The z-adiabatic modes obviously possess the symmetry property

$$\phi_\nu(x, z) = \wp_\nu \phi_\nu^*(-x, z). \tag{A38}$$

Hence we may write

$$C_\nu(z) = C_\nu^R(z) = \wp_\nu C_\nu^{L*}(z). \tag{A39}$$

The Wronskian formula (A29) becomes then

$$
\begin{aligned}
W(z) &= \sum_\nu \wp_\nu \left(C_\nu^*(z) \, i \, \partial_z \, C_\nu(z) - C_\nu(z) \, i \, \partial_z \, C_\nu^*(z) \right) \\
&\quad + \sum_{\nu\nu'} (\wp_\nu C_\nu^*(z) \, C_{\nu'}(z) \, i \, (\phi_\nu|\partial_z\phi_{\nu'})_x \\
&\quad - \wp_{\nu'} \, C_\nu(z) \, C_{\nu'}^*(z) \, i \, (\phi_\nu|\partial_z\phi_{\nu'})_x) \\
&= \sum_\nu \wp_\nu \left(C_\nu^*(z) \, i \, \partial_z \, C_\nu(z) - C_\nu(z) \, i \, \partial_z \, C_\nu^*(z) \right) \\
&\quad + \sum_{\nu\nu'} \wp_\nu C_\nu^*(z) \, C_{\nu'}(z) \, 2 \, i \, (\phi_\nu|\partial_z\phi_{\nu'})_x. \quad (A40)
\end{aligned}
$$

The last line of Eq. (A40) is granted to be real valued, since

$$
\begin{aligned}
&\sum_{\nu\nu'} \wp_\nu C_\nu^*(z) \, C_{\nu'}(z) \, 2 \, i \, (\phi_\nu|\partial_z\phi_{\nu'})_x \\
&= \sum_{\nu\nu'} \wp_{\nu'} C_{\nu'}^*(z) \, C_\nu(z) \, 2 \, i \, (\phi_{\nu'}|\partial_z\phi_\nu)_x \\
&= \sum_{\nu\nu'} \wp_{\nu'} C_{\nu'}^*(z) \, C_\nu(z) \, 2 \, (-i) \, (\phi_\nu|\partial_z\phi_{\nu'})_x \\
&= \sum_{\nu\nu'} C_{\nu'}^*(z) \, C_\nu(z) \, 2 \, (-i) \, \wp_\nu \, (\phi_\nu|\partial_z\phi_{\nu'})_x^* \\
&= \left(\sum_{\nu\nu'} \wp_\nu C_\nu^*(z) \, C_{\nu'}(z) \, 2 \, i \, (\phi_\nu|\partial_z\phi_{\nu'})_x \right)^*. \quad (A41)
\end{aligned}
$$

We have taken advantage here of the following identity:

$$
\begin{aligned}
(\phi_\nu|\partial_z\phi_{\nu'})_x &= \int_{-\infty}^{+\infty} dx \, \phi_\nu(x,z)\partial_z \, \phi_{\nu'}(x,z) \\
&= \int_{-\infty}^{+\infty} dx \, \phi_\nu(-x,z)\partial_z \, \phi_{\nu'}(-x,z) \\
&= \wp_\nu \wp_{\nu'} \int_{-\infty}^{+\infty} dx \, \phi_\nu^*(x,z)\partial_z \, \phi_{\nu'}^*(x,z) \\
&= \wp_\nu \wp_{\nu'} \, (\phi_\nu|\partial_z\phi_{\nu'})_x^*. \quad (A42)
\end{aligned}
$$

Equations (A36), (A37), and (A40) have proven to be very useful for checking the accuracy of our numerical calculations presented in the main text.

Finally, for the sake of completeness and clarity, let us supply one little addition: In the Hermitian *and* symmetric case we have both $n(x, z) = n^*(x, z)$ *and* $n(x, z) = n^*(x, z)$. Correspondingly, we encounter *two* distinct conserved (z-independent) Wronskian entities: The first is the one derived

in Appendix A 2, which reads as

$$
\begin{aligned}
W(z) = &\int_{-\infty}^{+\infty} dx \\
&\times \Psi_R^*(+x, z) \, i \, \partial_z \, \Psi_R(x, z) \\
&- \Psi_R(x, z) \, i \, \partial_z \, \Psi_R^*(+x, z), \quad (A43)
\end{aligned}
$$

or equivalently

$$
\begin{aligned}
W(z) &= \sum_\nu \left(C_\nu^*(z) \, i \, \partial_z \, C_\nu(z) - C_\nu(z) \, i \, \partial_z \, C_\nu^*(z) \right) \\
&\quad + \sum_{\nu\nu'} C_\nu^*(z) \, C_{\nu'}(z) \, 2 \, i \, (\phi_\nu|\partial_z\phi_{\nu'})_x. \quad (A44)
\end{aligned}
$$

The second is the Wronskian entity (A37) and Eq. (A40) derived above.

APPENDIX B: SOME ADDITIONAL PLOTS

Here we supply some additional plots complementing the results presented in the main text.

1. Straight WGs, $\alpha(1000 \, \mu\mathrm{m}) = 0.148 \, \mu\mathrm{m}^{-1}$ $[\alpha_{\mathrm{EP}}(1000 \, \mu\mathrm{m}) = 0.150 \, \mu\mathrm{m}^{-1}]$

Figure 8 shows the used profile of $\alpha(z)$. Figures 9 and 10 show that the off-diagonal nonadiabatic couplings [cf. Eqs. (7) and (8) of the main paper] are almost zero around $z = 1000 \, \mu\mathrm{m}$ where the EP is approached. Therefore, one may expect that the $\mathcal{PT}$ symmetry will be well preserved around $z = 1000 \, \mu\mathrm{m}$ in close vicinity of the EP. Such an expectation is confirmed by the upper panel of Fig. 6 of the main paper. Figure 11 shows the calculated expansion coefficients $C_\nu(z)$ entering into Eq. (4) of the main text.

2. Straight WGs, $\alpha(1000 \, \mu\mathrm{m}) = 0.14975 \, \mu\mathrm{m}^{-1}$ [closer to $\alpha_{\mathrm{EP}}(1000 \, \mu\mathrm{m}) = 0.150 \, \mu\mathrm{m}^{-1}$]

Figure 12 shows the used profile of $\alpha(z)$. Figures 13 and 14 show that the off-diagonal nonadiabatic couplings [cf. Eqs. (7) and (8) of the main paper] are reduced around $z = 1000 \, \mu\mathrm{m}$ where the EP is approached. Therefore, one may expect that the $\mathcal{PT}$ symmetry will be approximately preserved around $z = 1000 \, \mu\mathrm{m}$ in close vicinity of the EP. Such an expectation is confirmed by the lower panel of Fig. 6 of the main paper. Figure 15 shows the calculated expansion coefficients $C_\nu(z)$ entering into Eq. (4) of the main text.

3. Bent WGs, $\alpha(1000 \, \mu\mathrm{m}) = 0.148 \, \mu\mathrm{m}^{-1}$

Figure 16 shows that a slight bending of the studied WGs (which cannot be avoided in experiments) would affect only marginally the output signal. On the other hand, a larger bending (performed possibly by an eavesdropper in order to allow for tapping light) leads to a dramatic (exponential) enhancement or suppression of the output signal.

[1] W. D. Heiss, J. Phys. A **45**, 444016 (2012).

[2] L. Feng, R. El-Ganainy, and L. Ge, Nat. Photonics **11**, 752 (2017).

[3] R. El-Ganainy, K. G. Makris, M. Khajavikhan, Z. H. Musslimani, S. Rotter, and D. N. Christodoulides, Nat. Phys. **14**, 11 (2018).

[4] S. K. Özdemir, S. Rotter, F. Nori, and L. Yang, Nat. Mater. **18**, 783 (2019).

[5] M.-A. Miri and A. Alu, Science **363**, eaar7709 (2019).

[6] D. F. P. Pile, Nat. Photonics **11**, 742 (2017).

[7] B. Midya, H. Zhao, and L. Feng, Nat. Commun. **9**, 2674 (2018).

[8] R. El-Ganainy, M. Khajavikhan, D. N. Christodoulides, and S. K. Özdemir, Commun. Phys. **2**, 37 (2019).

[9] Y. Berlatzky, I. Shtrichman, R. Narevich, E. Narevicius, G. Rosenblum, and I. Vorobeichik, J. Lightwave Technol. **23**, 1278 (2005).

[10] Y. Berlatzky, I. Shtrichman, R. Narevich, E. Narevicius, G. Rosenblum, and I. Vorobeichik, IEEE J. Quantum Electron. **42**, 477 (2006).

[11] K. G. Makris, R. El-Ganainy, D. N. Christodoulides, and Z. H. Musslimani, Phys. Rev. Lett. **100**, 103904 (2008).

[12] S. Klaiman, U. Günther, and N. Moiseyev, Phys. Rev. Lett. **101**, 080402 (2008).

[13] C. E. Rüter, K. G. Makris, R. El-Ganainy, D. N. Christodoulides, M. Segev, and D. Kip, Nat. Phys. **6**, 192 (2010).

[14] A. Szameit, M. C. Rechtsman, O. Bahat-Treidel, and M. Segev, Phys. Rev. A **84**, 021806(R) (2011).

[15] S. Weimann, M. Kremer, Y. Plotnik, Y. Lumer, S. Nolte, K. G. Makris, M. Segev, M. C. Rechtsman, and A. Szameit, Nat. Mater. **16**, 433 (2017).

[16] W. E. Hayenga *et al.*, ACS Photonics **6**, 1895 (2019).

[17] A. L. M. Muniz, M. Wimmer, A. Bisianov, U. Peschel, R. Morandotti, P. S. Jung, and D. N. Christodoulides, Phys. Rev. Lett. **123**, 253903 (2019).

[18] J. Zheng, X. Yang, D. Deng, and H. Liu, Opt. Express **27**, 1538 (2019).

[19] M. Sakhdari, M. Hajizadegan, Q. Zhong, D. N. Christodoulides, R. El-Ganainy, and P.-Y. Chen, Phys. Rev. Lett. **123**, 193901 (2019).

[20] N. S. Nye, A. E. Halawany, C. Markos, M. Khajavikhan, and D. N. Christodoulides, Phys. Rev. Appl. **13**, 064005 (2020).

[21] N. Moiseyev and A. Mailybayev, in *Parity-Time Symmetry and its Applications*, edited by D. Christodoulides and J. Yang (Springer, Berlin, 2018).

[22] N. Moiseyev, *Non-Hermitian Quantum Mechanics* (Cambridge University Press, Cambridge, U.K., 2011).

[23] P. Jensen and P. R. Bunker, *Computational Molecular Spectroscopy* (Wiley, New York, 2000).

[24] The bend section in optical circuits supports only leaky modes. The minimal arc radius in the optical circuit is determined by the maximal allowable loss per unit arc length. See Y. Berlatzky, Ph.D. thesis. Technion, 2007, https://www.graduate.technion.ac.il/Theses/Abstracts.asp?Id=24091.

[25] T. Goldzak, A. A. Mailybaev, and N. Moiseyev, Phys. Rev. Lett. **120**, 013901 (2018).

[26] F. Ladoucer and P. Labeye, J. Lightwave Technol. **13**, 481 (1995).

[27] M. Heiblum and J. H. Harris, IEEE J. Quantum Electron. **11**, 75 (1975).

[28] B. Friedrich and D. Herschbach, J. Phys. Chem. A **103**, 10280 (1999).

[29] N. Moiseyev and A. K. Gupta, Mol. Phys. **110**, 1721 (2012).

[30] https://metavo.metacentrum.cz.

[31] I. Vorobeichik, N. Moiseyev, and D. Neuhauser, J. Opt. Soc. Am. B **14**, 1207 (1997).